Revista Brasileira de Geografia Física v.17, n.1 (2024) 297-314.

ISSN:1984-2295

Revista Brasileira de Geografia Física

Homepage:https://periodicos.ufpe.br/revistas/rbgfe

Morphometry, Water Availability and Sediment Transport in the River Renato Watershed, Southern Amazon

Daniela Roberta Borella[1], Daniela Castagna[2], Alexandre Claro Garcia[1], Marco Aurélio Barbosa Alves[3], Cornélio Alberto Zolin[4], Frederico Terra de Almeida[5], Adilson Pacheco de Souza[5]*

[1] Pós-Doutoranda(o) em Ciências Ambientais, Universidade Federal de Mato Grosso (UFMT), Avenida Alexandre Ferronato, Distrito Industrial, nº1200, CEP 78550-728, Sinop, Mato Grosso, Brasil. (66) 3533-3116. drborella@gmail.com. [2] Doutoranda em Física Ambiental, Universidade Federal de Mato Grosso – UFMT, Avenida Fernando Corrêa da Costa, Cidade Universitária, nº 2367, CEP 78060-900, Cuiabá, Mato Grosso, Brasil. (65) 3313 7306. danicastagna.geo@gmail.com. [3] Doutorando em Agronomia (Ciências do Solo), Universidade Federal Rural do Rio de Janeiro, Instituto de Agronomia, Km 07, Zona Rural, BR-465, Seropédica - RJ, 23890-000. marcoaurelio.monitor@gmail.com.br. [4] Pesquisador, Dr., Empresa Brasileira de Pesquisa Agropecuária, Embrapa Agrossilvipastoril – EMBRAPA, Rodovia MT 222, Km 2,5, s/n, CEP 78550-970, Sinop, Mato Grosso, Brasil. (66) 3211-4220. cornelio.zolin@embrapa.br. [5] Professor Dr., Universidade Federal de Mato Grosso (UFMT), Avenida Alexandre Ferronato, Distrito Industrial, nº1200, CEP 78550-728, Sinop, Mato Grosso, Brasil. (66) 3533-3116. fredterr@gmail.com, pachecoufmt@gmail.com (*autor correspondente).

Artigo recebido em 21/07/2023 e aceito em 25/12/2023

A B S T R A C T

The reduction in surface water availability in the Brazilian Amazon biome is associated with anthropic activities and climate change, facts that have driven hydrological monitoring studies. Such studies seek to understand the hydrological responses to changes in land use and land cover, aiming to properly manage water resources in Amazonian river basins. Thus, the objective of the present study was to determine the physiographic characteristics and establish liquid and solid rating curves of the Renato river sub-basin, a tributary of the Teles Pires river, under conditions of restricted data. Measurements of quota, liquid flow (Q_L) and solid flows in suspension (Q_{ss}) and drag (Q_{sa}) took place monthly between February 2019 and November 2022, composing 28 and 16 (fluviometric station 1) and 21 and 16 (station fluviometric 2) measurements of Q_L, Q_{ss} and Q_{sa}, respectively. Physiographic characteristics were determined using the QGIS 3.16.11 software. The Renato River sub-basin had a regular drainage density = 0.505 km km^{-2}, an elongated shape and low probability of flooding (K_f = 0.19; K_c = 2.17 and I_c = 0.21) and the relief varied from flat to strongly undulating (0 to 30%). The different regression models adjusted for Q_L showed satisfactory statistical performance; the hydrological section 1 obtained mean values of Q_L = 1.52 m^3 s^{-1}, Willmott concordance index (dw) = 0.8999, Nash-Sutcliffe efficiency (NSE) = 0.60 and slight underestimation of Q_L, hydrological section 2 obtained mean values of Q_L = 18.09 m^3 s^{-1}, dw = 0.9599, NSE = 0.83 and small overestimate of Q_L. Regardless of the hydrological section, the statistical performance of the regression models for suspended and total solid flows (Q_{st}) could have been better. It is concluded that the Renato River watershed is little susceptible to extreme flood events due to its elongated shape and regular drainage density. The evaluated regression models adjusted satisfactorily for Q_L and unsatisfactorily for Q_{ss} and Q_{st}. Therefore, there is still a need to continue studies with hydrosedimentological monitoring to build rating curves that accurately estimate the liquid and solid flows.

Keywords: physiographic characteristics, hydrosedimentological monitoring, Teles Pires river, rating curves.

Morfometria, Disponibilidade Hídrica e Transporte de Sedimentos na Bacia Hidrográfica do Rio Renato, Sul da Amazônia

R E S U M O

A redução da disponibilidade hídrica superficial no bioma Amazônia brasileiro está associada as atividades antrópicas e mudanças climáticas, fatos que tem impulsionado os estudos de monitoramento hidrológico. Tais estudos, buscam compreender as respostas hidrológicas frente as mudanças de uso e cobertura da terra visando a adequada gestão dos recursos hídricos em bacias hidrográficas amazônicas. Assim, o objetivo do presente estudo foi determinar as características fisiográficas e estabelecer curvas-chave líquida e sólidas da sub-bacia hidrográfica do rio Renato, afluente do rio Teles Pires, sob condições de dados restritos. As medidas de cota, vazão líquida (Q_L) e vazões sólidas em suspensão (Q_{ss}) e de arrasto (Q_{sa}) ocorreram mensalmente entre fevereiro de 2019 e novembro de 2022, compondo 28 e 16 (estação fluviométrica 1) e 21 e 16 (estação fluviométrica 2) medições de Q_L, Q_{ss} e $Q_{sa,}$ respectivamente. As características fisiográficas foram determinadas utilizando o software QGIS 3.16.11. A sub-bacia hidrográfica do rio Renato apresentou

densidade de drenagem regular = 0,505 km km^{-2}, forma alongada e com baixa probabilidade de ocorrência de enchentes (k_f = 0,19; k_c = 2,17 e I_c = 0,21) e o relevo variou de plano a fortemente ondulado (0 a 30%). Os diferentes modelos de regressão ajustados para Q_L apresentaram desempenho estatístico satisfatório, a seção hidrológica 1 obteve valores médios de Q_L = 1,52 m^3 s^{-1}, índice de concordância de Willmott (dw) = 0,8999, eficiência de Nash-Sutcliffe (NSE) = 0,60 e pequena subestimativa de Q_L, a seção hidrológica 2 obteve valores médios de Q_L = 18,09 m^3 s^{-1}, dw = 0,9599, NSE = 0,83 e pequena superestimativa de Q_L. Independentemente da seção hidrológicas, o desempenho estatístico dos modelos de regressão para as vazões sólidas em suspensão e total (Q_{st}) foram insatisfatório. Conclui-se que a sub-bacia hidrográfica do rio Renato é pouco susceptível aos eventos extremos de enchentes, devido sua forma alongada e densidade de drenagem regular. Os modelos de regressão avaliados ajustaram de forma satisfatória para Q_L e insatisfatória para Q_{ss} e Q_{st}. Portanto, ainda há necessidade de continuar os estudos com monitoramento hidrossedimentológico para construir curvas-chave que estimam de forma acurada as vazões líquida e sólida.
Palavras-chave: características fisiográficas, monitoramento hidrossedimentológico, rio Teles Pires, curvas-chaves.

Introduction

The intensification of conflicts over the consumptive and non-consumptive uses of water has impacted the different production chains, society's quality of life and the maintenance of natural ecosystems. Water is an indispensable natural resource to meet the multiple demands of human and industrial supply, animal watering, agricultural irrigation, collection or discharge of effluents, energy generation, recreation, tourism, navigation, maintenance of natural ecosystems, among others (Stinghen & Mannich, 2022). In this sense, conducting studies aimed at hydrological monitoring is essential to identify this natural resource's quantitative and qualitative availability and support the proper management of water resources.

Brazil has about 6% of the surface and 12% of the volume of fresh water on the planet, of which around 78% are rivers and natural lakes and 22% are reservoirs and artificial dams (MapBiomas, 2021). In the mapping of surface water in Brazil, between 1985 and 2020 carried out by MapBiomas, a significant reduction in surface water availability was recorded in all regions/biomes of the country, despite some gains in surface water that are predominantly associated with the installation of hydroelectric projects.

In the state of Mato Grosso, there was a reduction in the water surface between 1990 and 2020 (MapBiomas, 2021). This reduction in surface water availability is associated with land use and land cover changes, above all, the conversion of natural vegetation into agricultural and urban areas (Lopes et al., 2021; Kraeski et al., 2022). These changes, in turn, influence the hydrological components, causing a reduction in the volume of precipitated water and evapotranspiration (Santos et al., 2019).

The hydrological regime of a region or of the watersheds that make up an area is dependent on climatic conditions (Groppo et al., 2019; Rodrigues et al., 2020), soil geomorphology (Wenzel et al., 2017; Santos et al., 2019) and the type of vegetation cover (Souza et al., 2019; Peixoto et al., 2020). Among these variables, changes in land use and land cover can generate faster changes in hydro-sedimentological processes since climate variations are associated with extreme events and their influence on hydrological components are also dependent on the morphometric characteristics of the watershed.

Therefore, the absence of conservation practices in arable soils and the suppression of natural vegetation influence the infiltration capacity, storage and drainage of rainwater in the soil and the rates of production and transport of sediments in watersheds (Souza et al., 2019; Peixoto et al., 2020). In addition, there are numerous negative impacts generated by the transport of high concentrations of sediments, such as pollution of water bodies, reduction and extinction of aquatic species (Andrietti et al, 2016; Wang et al., 2016), impoverishment of arable soils with the loss of the surface layer, silting and greater susceptibility to the formation of floods, changes in the volume and flow of water, the morphology of the bed and the basin margin s hydrographic (Zhanga et al., 2019), decrease in the useful life of works, reservoirs, abrasion of turbines and other equipment (Ziembowicz et al., 2018).

In hydrosedimentological monitoring, continuous measurements of the components of the hydrological cycle in the watersheds should be carried out, with greater emphasis on the monitoring of water level and turbidity, which allow for determining the volume of surface water (liquid flow) and the production and transport of sediments (solid flow). These two variables are dependent on rainfall characteristics (intensity, depth, duration, frequency and pattern of occurrence), vegetation cover, soil, climate (Almeida et al., 2019; Sousa et al., 2020) and the physiographic characteristics of the watershed (Wenzel et al., 2017; Santos et al., 2019). In this case, it is noteworthy that the transport and deposition of sediments are still dependent on the shape, size and mass of the particles, in addition to the slope, morphology and surface runoff velocity of watercourses (Lepesqueur et al., 2019; Peixoto et al., 2021).

The in-loco measurement of liquid flow and the sampling of sediments in natural watercourses are fundamental for defining rating curves and calibrating hydrological models, which allow predictions of flood events, water scarcity, soil loss and reservoir silting up. In addition, they can help in the adoption of mitigating measures for these problems, such as the implementation of adequate land management practices (Lopes et al., 2021; Berihun et al., 2022), the definition of hydro-agricultural and forestry projects (Zolin et al., 2016), the regulation of outflows in reservoirs (Uliana et al., 2016) and the control of production, transport and deposition of sediments (Simioni et al., 2021; Marinho et al., 2022; Sirqueira et al., 2022).

In the regional context, gathering hydrological information on surface water availability and sediment transport in small natural watercourses is essential since the most excellent anthropic demands occur in watercourses with a smaller drainage area, as is the case of rivers and streams in the southern Amazon and northern Mato Grosso. The scarcity of hydrological information on tributaries of the Teles Pires river basin has motivated studies on the hydrological dynamics and continuous monitoring of perennial channels and drainage networks with a small degree of branching to support the planning and adequate management of water and soil in this region.

In this sense, this paper aimed to determine the physiographic characteristics and establish the rating curves of liquid flow and sediments in the Renato River sub-basin, a tributary of the Teles Pires River. This hydrographic sub-basin still has a high percentage of natural vegetation (native forests) compared to other regional sub-basins. However, it has recently changed land use due to the opening of new areas (deforestation) and crop replacement of pasture areas.

Material and methods

Characterization of the study region

The study area corresponds to a watershed belonging to the hydrographic basin of the Teles Pires River, which, in turn, is located between latitudes 7º 16' 47'' and 14º 55' 17'' S and longitudes 53º 49' 46'' and 58º 07' 58'' W, covering the territories of the states of Mato Grosso and Pará, Brazil. The drainage area of the basin of the Teles Pires River is around 141,278 km², and the length of the main waterway is approximately 1,498 km. This hydrographic basin is inserted in the agribusiness pole region of Mato Grosso. It has the predominant vegetation cover of the Cerrado (upper Teles Pires) and Amazon (middle and lower Teles Pires) biomes (Figure 1).

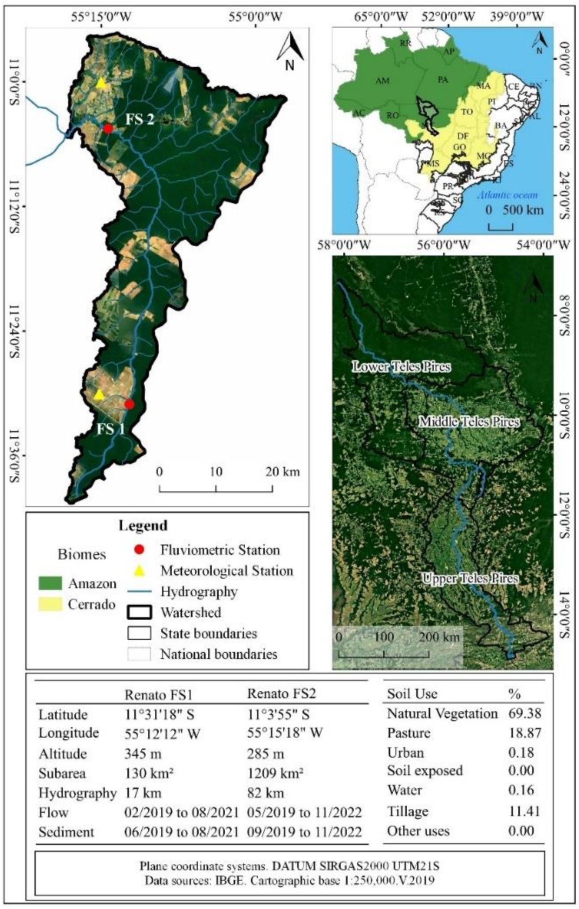

	Renato FS1	Renato FS2
Latitude	11°31'18" S	11°3'55" S
Longitude	55°12'12" W	55°15'18" W
Altitude	345 m	285 m
Subarea	130 km²	1209 km²
Hydrography	17 km	82 km
Flow	02/2019 to 08/2021	05/2019 to 11/2022
Sediment	06/2019 to 08/2021	09/2019 to 11/2022

Soil Use	%
Natural Vegetation	69.38
Pasture	18.87
Urban	0.18
Soil exposed	0.00
Water	0.16
Tillage	11.41
Other uses	0.00

Figure 1. Location map of the fluviometric and meteorological stations and principal land uses of the River Renato sub-basin, a tributary of the River Teles Pires Watershed, Southern Amazon, Mato Grosso, Brazil. Note: in the general information table of the fluviometric stations, the period of punctual measurements (monthly) of the liquid and solid flows is presented. Source: Land Uses (MapBiomas, 2020).

The Renato River watershed is located on the right bank and in the region of the middle Teles Pires River, in southern Amazonia, between latitudes 11°40'35.57'' S and 10°55'17.28'' S and longitudes 55°18'17.25'' W and 54°56'59.69'' W. The drainage area of this watershed is about 1,336 km², and the length of the main waterway is approximately 95 km (Figure 1). The watershed area is covered with about 69% of natural vegetation and the main economic activities are concentrated in timber and non-timber forest management, extensive livestock and a significant rise in agriculture (Figure 1).

The climate in the region is Aw (tropical hot and humid), with climatic seasonality defined by two water seasons, the rainy (October to April) and dry (May to September). The average annual precipitation is 1,970 mm and the average monthly temperatures vary between 24 and 27 °C (Souza et al., 2013). During the evaluation period, the study region accumulated an average annual rainfall of 1,915 mm and an average monthly air temperature between 25 and 27 °C (Figure 2), corroborating what was observed by Souza et al. (2013).

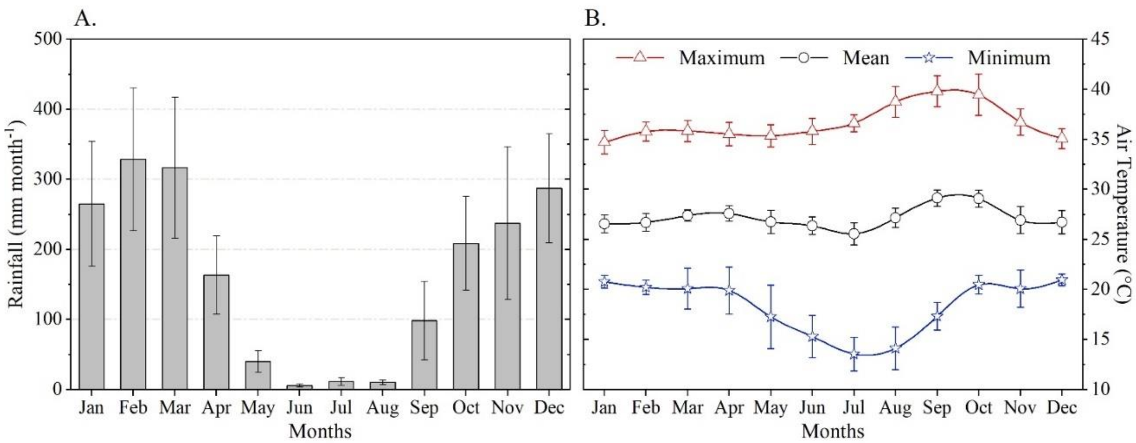

Figure 2. Monthly means and standard deviations for rainfall (A) and air temperature (B) in the study region of the River Renato Watershed, Southern Amazon, Mato Grosso, Brazil. Source: Agrometeorological Monitoring System (Agritempo, 2022).

According to the Brazilian Institute of Geography and Statistics - IBGE, the most recurrent soils in the Renato River watershed are Plinthsols and Oxisols (IBGE, 2021). Alves et al. (2022) describe that the Oxisols of this watershed range from Red to Red-Yellow, all dystrophic, with a more clayey texture in the upper region (source) and medium texture in the lower regions (mouth). In general, Oxisols have characteristics that respond well to fertilization for tropical crops. This description of soil classification also corroborates the study by Spera et al. (2019) in forest soils in the region of the mouth of the Renato River watershed.

Physiographic characteristics

The Digital Elevation Model (DEM) based on data from the SRTM (Shuttle Radar Topography Mission) with a spatial resolution of 90 x 90 meters was used as a database to obtain the physiographic characteristics. Vector data were obtained from the cartographic base of IBGE (2017) at a scale of 1:250,000. Data processing and getting the morphometric variables of the Renato River watershed were performed using the QGIS 3.16.11 software.

The drainage area (Ad, in km^2), perimeter (P, in km), and axial length (Laxial, in km) were obtained after the delimitation of the Renato River watershed. The length of the main watercourse (Lp, in km) and its thalweg ($L_{talvegue}$, in km), the total length of the drainage network (L_{total}, in km), and the number of watercourses were obtained after extracting the sub-basin drainage network. Finally, the amplitudes of altitude (in meters) and slope (in %) were extracted from the DEM of the watershed.

From obtaining the aforementioned morphometric variables, the physiographic indicators form factor (K_f) (Equation 1), compactness coefficient (Kc) (Equation 2), circularity index (Ic) (Equation 3), sinuosity (S) (Equation 4) and drainage density (Dd, in km km^{-2}) (Equation 5) were calculated, according to Wenzel et al. (2017):

$$K_f = \frac{A_d}{{L_{axial}}^2} \quad \text{(Equation 1)}$$

$$K_C = 0.28 * \frac{P}{\sqrt{A_d}} \quad \text{(Equation 2)}$$

$$I_C = \frac{12.57 * A_d}{P^2} \quad \text{(Equation 3)}$$

$$S = \frac{L_P}{L_{talvegue}} \qquad \text{(Equation 4)}$$

$$D_d = \frac{L_{total}}{A_d} \qquad \text{(Equation 5)}$$

where: K_f is the shape factor (dimensionless); Ad is the drainage area (km^2); L_{axial} is the axial length of the watershed (km); Kc is the compactness coefficient (dimensionless); P is the watershed perimeter (km); It is the roundness index (dimensionless); S is the sinuosity (dimensionless); Lp is the length of the main watercourse (km), Ltalweg is the length of the thalweg of the main watercourse (km), Dd is the drainage density (km km^{-2}); Ltotal is the length of all watercourses in the watershed (km).

The Kf, Kc, Icand S indices are dimensionless and vary according to the shape of the watershed. Kf can be classified as: from 1.00 to 0.75; from 0.75 to 0.50; and ≤ 0.5, which represent high, median, and low probability (susceptibility) to significant floods, respectively. Kc varies as follows: 1.00 ≤ Kc <1.25; 1.25 ≤ Kc <1.50 and Kc ≥ 1.50, representing high, median and low probability of major floods, respectively. The circularity index presents the following variation: Ic ≥ 0.51 and Ic < 0.51, indicating that the basin is circular or elongated. The Dd indicates that the watershed can present poor drainage (Dd < 0.5 km km-2), regular (0.5 ≤ Dd < 1.5 km km^{-2}), good (1.5 ≤ Dd < 2.5 km km^{-2}), excellent (2.5 ≤ Dd < 3.5 km km^{-2}) and exceptionally well drained (Dd ≥ 3.5 km km^{-2}) (Mello, 2013; Santos et al., 2019).

Monitoring fluviometric sections

The definition of fluviometric stations 1 and 2 of the Renato River watershed (Figure 3) for hydrological and sedimentological monitoring was carried out seeking to follow the criteria described by Santos et al. (2001) such as: ease of access and logistics, site free of anthropic actions, stretch with well-distributed speeds, stable bed and bank, well defined and free of vegetation, rocks and other obstacles, straight section with parallel banks, regular longitudinal profile and free of backwaters and location far from confluences, location with adequate conditions for installation, maintenance and operation of equipment.

The fluviometric stations were instrumented with sets of linimetric rulers with a numerical scale of 0.02 m and a level sensor with a buoy and counterweight system. This sensor continuously measures water level variation at 10-minute intervals, converting mechanical pulses into electrical signals interpreted by an external data logger (programmable logic controller). This equipment was installed on the margins of each cross section following the ANA recommendations (2021).

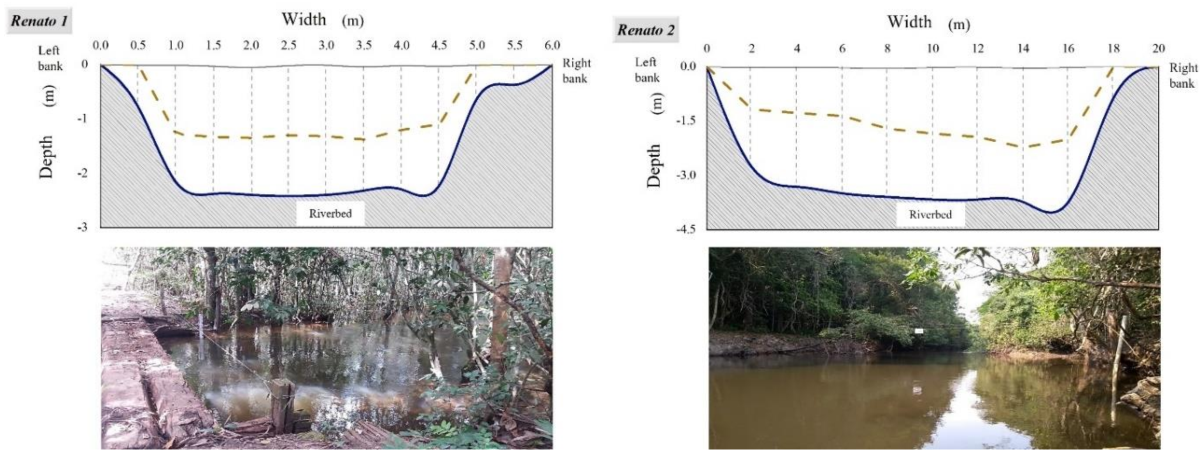

Figure 3. Cross sectional profiles of the hydrological sections on the River Renato Watershed, demonstrating the width, depth, distance between verticals and the number of verticals of each cross-section in the dry season (dashed brown line) and rainy season (solid blue line).

Flow measurements to establish the rating curve

The monitoring cross-sections were demarcated with a graduated rope fixed between the channel margins and then divided into subsections, represented by fixed verticals, positioned longitudinally along the section. The distance between verticals and the number of verticals were defined according to the width of each cross section. In contrast, the position and number of reading points were determined from the depth measurement of each vertical, according to the criteria established by Santos et al. (2001). The position and number of verticals and measuring points may vary according to the year's water season, which is necessary to measure the width and depth of the fluviometric cross sections at each field campaign (Figure 3).

Liquid flow measurements in cross section 1 of the Renato River with vertical depths of less than 2.50 m were carried out at ford, with the aid of a metallic rod graduated with a numerical scale of 0.01 m, the river bed being the reference (obtaining H - height of the water column above the point). In cross section 2 of the Renato river with a vertical depth greater than 2.50 m, a complete fluviometric winch (model *GFL-25*) and a fluviometric ballast (model *LAS-15*), installed in an aluminum boat and a 15hpa squash engine were used. In this method, the reference is the surface of the water, and an analog odometer is used, which must be zeroed with the central axis of the hydrometric windlass leveled with the surface of the water, and, subsequently, submerged to the riverbed to obtain the P (depth) of the vertical.

The liquid flow measurements were carried out by direct measurement with a hydrometric windlass, model *MLN-7*, associated with an electronic revolution counter, connected to each other. In this case, the metal propeller rotates in the opposite direction of the flow under the action of the movement of the water in the river. It sends electrical signals to the rotation counter, which relates the number of rotations per second to the flow velocity.

During the measurements, the equipment was positioned with the propeller positioned against the water flow direction and three readings of the number of rotations were performed, for a time of 40 s per reading, considering a standard deviation ≤ 10%, in each position of each vertical of the cross section, from the left bank to the right bank. To obtain the average speed in each vertical, the rotations were converted into rates through the linear equation established by the manufacturer. The time of 40 s per reading was sufficient for average regular flow conditions in all sections evaluated as Santos et al. (2001) recommended.

The wet area of influence of the cross sections was calculated using the numerical method of the half section or subsection, which consists of calculating the partial flows of each subsection by multiplying the average velocity of the vertical by the area of the trapezoidal segment, defined by the product of the average depth by the sum of the semi-distances to the adjacent verticals (Santos et al., 2001). This method disregards the areas close to the margins (Equation 6). The total net flow for each cross section was determined by the sum of the product of velocity and wetted area of each subsection (Equation 7).

$$A_i = \frac{\left(\frac{P_{i-1} + P_i}{2} + P_i\right)}{2} \cdot \frac{(d_i - d_{i-1})}{2} + \frac{\left(P_i + \frac{P_{i+1} + P_i}{2}\right)}{2} \cdot \frac{(d_{i+1} - d_i)}{2}$$
(Equation 6)

where: P_{i-1} is the depth of the vertical preceding the vertical whose area of influence is being calculated (m); P_i is the depth of the vertical whose area of influence is being calculated (m); P_{i+1} is the depth of the vertical behind the vertical whose influence area is being calculated (m); $d_i – d_{i-1}$ is the distance between the vertical whose area of influence is being calculated and the previous vertical (m); $d_{i+1} – d_i$ is the distance between the vertical whose area of influence is being calculated and the posterior vertical (m).

$$Q_L = \sum q_i = \sum (V_i * A_i)$$ (Equation 7)

where: Q_L is the total net flow ($m^3 s^{-1}$); q_i is the flow of each subsection ($m^3 s^{-1}$); V_i is the average velocity of the vertical ($m s^{-1}$) and A_i is the wetted area of the subsection (m^2).

A sampling of sediments to establish the rating curve

The sampling method of equal width increment – IIL (Carvalho, 2008) was adopted to collect suspended sediments in the two monitoring cross sections. In this case, the transverse sections were divided into segments or subsections or verticals of equal width, allowing samples of water and suspended sediments to be obtained in each subsection or vertical. This method was chosen based on prior knowledge of the distribution of velocity and net flow of each cross section and also because it is a recommended method for simplifying the methodology in the field and analysis of results (Carvalho, 2008; Simioni et al., 2021; Peixoto et al., 2021).

In applying the IIL method, indirect measurement of suspended sediments was used with vertical integration sampling. This methodology consists of obtaining a sample of water plus sediments in suspension, along the vertical, with a uniform transit velocity. In this case, the equipment used was the *US DH-48* and *US D-49* suspended sediment samplers; both samplers have 1/8", 3/16" and 1/4" diameter nozzles and a non-sampled zone of 0.09 and 0.10 m, respectively.

The choice of the samplers nozzle depended on the transit speed, which was defined by the time of ascent and descent of the equipment in the sampling by vertical integration. Then, sample collection efficiency tests were carried out with the three nozzles as mentioned above, considering the standard vertical descent and ascent (vertical with the greatest product of depth and velocity), using ratio 1: Vt / Vm = 0.2 for the 1/8" nozzle and ratio 2: Vt / Vm = 0.4 for the 3/16" and 1/4" nozzles. /4 to 4/5 of the collection bottle volume, standard upright.

The transit time and sample volume must differ in each vertical to maintain the same transit velocity (similar to water velocity) in cross section integration sampling. Therefore, the transit time for the standard vertical was calculated, and later for the other verticals (Carvalho, 2008). During sampling, the equipment's nozzle was kept horizontal, with the opening against the water flow, and avoiding contact with the river bed. These precautions prevented errors in the collection volume and contamination of the sample by sediment from drag.

Composite sampling (section) was carried out, which consisted of collecting about 1 L of sample volume (water and sediments) per vertical cross section. These samples were combined into a single sample (composite) with an approximate volume of 10 L. The volume of 10 L was determined based on the concentration of suspended sediment expected for the region, as recommended by the World Meteorological Organization (Carvalho, 2008).

Entrained sediments were sampled by direct measurement at the ford with rod using portable equipment model *US BLH-84* Helley Smith version. The equipment was positioned vertically at certain points of the bed in the cross section for 30 minutes and the opening was positioned in the direction of water flow. This sampler has a sampling efficiency close to 100% for sand and gravel, as it allows the collection of sediments to drag between 0.062 and 16 mm, through a nylon bag with a 0.2 mm mesh (Carvalho, 2008).

The entrained sediment samples were collected in a position of equal increment in width, in at least four verticals, chosen in an alternate position and distributed along each cross section according to the hydrodynamic characteristics, always avoiding verticals of static flow/still water. To avoid the loss of sediments, the samples were transferred to plastic bottles, washing a bag with distilled water, the containers were identified with the name of the monitoring section, date, type of sampling, vertical number and collection time for later processing of the samples (water and sediments from drag) in the laboratory.

The average concentration of suspended sediments per cross section (composite sample) was obtained by filtration in a vacuum polysulfone system, with porous membranes of 0.45 µm and a 0.5 L per filtration capacity. This method was chosen due to the low concentration of sediments in the rivers and streams studied.

Before filtration, the membranes were dried at 105 °C for about one hour and transferred to a hermetically sealed silica gel desiccator for weighing. At the beginning of each filtration, the suspended sediment samples were homogenized and filtered. The membranes were dried at 105 °C until a constant mass was obtained and then kept in the desiccator to avoid moisture exchange and to obtain the mass of the membrane set with dry sediments. The average concentration of suspended sediment per section was calculated by Equation 8.

Water samples with sediment from the trawl from each monitoring section were pooled and transferred to metal containers, with subsequent separation of the organic material before and after drying in an oven at 105 °C until constant mass or total water evaporation was obtained. The drying and weighing steps of suspended and entrained sediments were carried out using a forced air circulation oven and a 0.0001g precision digital scale, respectively.

The total solid flow was calculated by the sum of the solid flow in suspension sampled by cross section with the solid flow of drag (Equation 9). The solid drag flow was calculated by Equation 10; the solid flow in suspension was calculated by Equation 11.

$$C_{ss} = \frac{m_2 - m_1}{V} * 1000 \qquad \text{(Equation 8)}$$

where: Css is the suspended sediment concentration (mg L^{-1}); m1 is the mass of the clean and dry membrane (g); m_2 is the dry weight of the membrane with sediment (g); V is the volume of the sample (L).

$$Q_{st} = Q_{ss} + Q_{sa} \qquad \text{(Equation 9)}$$

$$Q_{sa} = \left[\frac{1440 * m * L}{E_{am} * n * l * t}\right] \quad \text{(Equation 10)}$$

$$Q_{ss} = 0.0864 * Q * C_{ss} \quad \text{(Equation 11)}$$

where: Q_{st} is the total solid flow (t d^{-1}); Qss is the suspended solid flow (t d^{-1}); Qsa is the solid drag flow (t d^{-1}); Q is the total net flow (m^3 s^{-1}); Css is the suspended sediment concentration (mg L^{-1}), all from each cross section; m is the mass of the total sample (t); L is the width of the cross section (m); Eam is the efficiency of the sampler for 30% of the bag = 1; n is the number of sampled verticals; l is the width of the sampler opening = 0.075 m and t is the sampling time (min).

Flow and sediment rating curves

In total, 28 and 21 measurements of liquid flow and water level in fluviometric stations 1 and 2, respectively, and 16 samples of solid discharges in suspension and drag were computed for each fluviometric station on a monthly scale between 2019 and 2022. The liquid and solid rating curves were adjusted for each cross section by testing different mathematical regression models (linear, polynomial, potential and exponential) (Table 1). To adjust the liquid key curve, the instantaneous measurements of the liquid flow were related to the water level readings obtained by the linimetric rulers, while to adjust the solid rating curves, the solid flows in suspension and total were related to the liquid flow, of each hydrological section.

In evaluating the performance of the adjusted models, the statistical indicators MBE - mean relative error (Equation 12); o RMSE - square root of mean relative error (Equation 13); and dw - Willmott concordance index (Equation 14) according to Souza et al. (2017); o NSE - Nash-Sutcliffe efficiency (Equation 15) according to Lopes et al. (2021) and Berihun et al. (2022) and Student's t-test for comparing two paired samples (Equation 16).

Table 1. Regression models fit the flow and sediment rating curves for hydrological sections 1 and 2 of the River Renato Watershed, Mato Grosso, Brazil.

Regression models	Equation
Linear	$y = a + b * x$
Polynomial	$y = a + b * x + c * x^2$
Potential I	$y = a * x^b$
Potential II	$y = a + b * x^c$
Potential III	$y = a * (x - b)^c$
Potential IV	$y = (a + b * x)^{(-1/c)}$
Potential V	$y = y_o + a * \lvert x - x_o \rvert^b$
Potential VI	$y = a * \lvert x - x_o \rvert^b$
Potential VII	$y = a * (1 + x)^b$
Exponential I	$y = a * (1 - \exp^{(-b*x)})$
Exponential II	$y = a * (1 - b^x)$
Exponential III	$y = \exp^{(a+b*x)}$
Exponential IV	$y = \exp^{(a+b*x+c*x^2)}$
Exponential V	$y = y_o + a * \exp^{(x-x_o)/b}$

Note: The equations highlighted in red were considered a reference for comparison with the other regression models.

The MBE calculates the average of the mean deviations between the observed and estimated values (model prediction), the RMSE provides the squared difference between the observed and estimated values, and the dw is a coefficient that indicates how much the values estimated by the model deviate from the observed mean. It has an interval between 0 and 1, where dw = 1 represents the complete adjustment between estimation and observation, and 0 indicates the opposite. The NSE is a normalized statistical coefficient that determines the relationship of the magnitude of the residual variance when compared with the variation of the measured data; its value can vary from -∞ to 1, where 1 indicates perfect fit of the model, NSE > 0.75 indicates very good performance, 0.65 < NS ≤ 0.75 indicates good performance, 0.50 < NS ≤ 0.65 indicates satisfactory performance, and NS ≤ 0.50

unsatisfied performance factor (Moriasi et al., 2007).

$$MBE = \frac{\sum_{i=1}^{n} P_i - O_i}{n} \quad \text{(Equation 12)}$$

$$RMSE = \left[\frac{\sum_{i=1}^{n} (P_i - O_i)^2}{n}\right]^{0.5} \quad \text{(Equation 13)}$$

$$dw = 1 - \frac{\sum_{i=1}^{n} (P_i - O_i)^2}{\sum_{i=1}^{n} (|P'_i - \bar{O}| + |O'_i - \bar{O}|)^2} \quad \text{(Equation 14)}$$

$$NSE = 1 - \frac{\sum_{i=1}^{n} (O_i - P_i)^2}{\sum_{i=1}^{n} (O_i - \bar{O})^2} \quad \text{(Equation 15)}$$

$$t = \frac{\bar{O}_i - \bar{P}_i}{\sqrt{\left(\frac{SD_{O_i}^{\,2}}{n}\right) + \left(\frac{SD_{P_i}^{\,2}}{n}\right)}} \quad \text{(Equation 16)}$$

where: P_i - estimated values; O_i - observed values; n - number of observations; $|P'_i - \bar{O}|$ - absolute value of the difference between the estimated value and the average of the observed values; $||O'_i - \bar{O}|$ - absolute value of the difference between the observed value and the average of the observed values; $\bar{P}_i$ – mean of estimated values; $\bar{O}_i$ – mean of observed values; SD – standard deviation.

Results

The drainage area of the Renato River is considered a hydrographic sub-basin of the Teles Pires River, of order 4 (IBGE, 2021). The Renato river watershed has regular drainage density, elongated shape and low probability of flooding. The relief is flat to strongly undulating, and the slope of the main watercourse between the source and the outlet is 0.12% (Table 2).

The cross sections of the Renato River watershed showed a stable bed and banks, trapezoidal in shape, with continuous and unidirectional flow and seasonal fluctuations in hydraulic variables (Table 3). The number of verticals ranged from 8 to 11 (cross section 1) and 8 to 9 (cross section 2) between the dry and rainy seasons, respectively, depending on the width of each section and the distance between verticals (Santos et al., 2001). Hydrological section 2 of the Renato river proportionally presented about 12 times more water volume drained by the main channel and solid flow in suspension when compared to hydrological section 1. In this case, it is noteworthy that section 2 has a drainage area 9.3 times greater than section 1 (Table 3).

Table 2. Physiographic characteristics of the River Renato Watershed, Southern Amazon, Mato Grosso, Brazil.

Physiographic characteristics	
Drainage area (km^2)	1,336.48
Perimeter (km)	283.38
Axial length (km)	83.6
Principal watercourse length (km)	94.6
Thalweg length of the principal watercourse (km)	63.49
The total length of watercourses (km)	674.37
Form factor - K_f	0.19
Compactness coefficient - K_c	2.17
Index circularity - I_c	0.21
Sinuosity - S	1.49
Drainage density ($km\ km^{-2}$)	0.505
Altitude range (m)	273 a 524
Slope range (%)	0 a 30
Principal watercourse slope to section 1 (%)	0.04
Principal watercourse slope to section 2 (%)	0.11
Sub-basin order	4
Total watercourses number	138

For hydrological section 1 of the Renato River, regardless of the regression model evaluated (linear, polynomial, potential and exponential), the statistical performance indicators showed satisfactory performance for the adjusted net rating curves, with small underestimation and reduced mean deviations, resulting in estimated values close to those observed in the field (Figure 4 and Table 4). Thus, the potential model, traditionally used to define the net rating curves of rivers, did not differ statistically from the other variations of the potential model and the other non-potential regressions. As for the solid rating curves, the evaluated regression models presented unsatisfactory statistical performances, with negative SES, low concordance indexes (dw), overestimates of the mean deviations close to the minimum values of solid discharge sampled during the evaluated period (Table 4).

These results can be explained by the low number of sediment samples and by the influence of other factors on the hydro-sedimentological dynamics of these cross-sections, such as temporal and spatial changes in land use, temporal and spatial distribution of heavy rainfall, among others. For the net flow, the MBE indicated an average underestimate of 0.1257 $m^3\ s^{-1}$, the Willmott adjustment index was greater than 0.8984 and the NSE ranged from 0.59 to 0.61 between the regression models. For solid flows in suspension and total, the MBE indicated an average overestimation of 0.1610 t d^{-1} and great scattering, the dw was on average 0.6296 for Q_{ss} and 0.6239 for Q_{st}, the Nash-Sutcliffe efficiency resulted in negative values, indicating the unsatisfactory performance of the tested models, on the other hand, there was no significant difference by the t-test between the values observed and estimated by the equations (Table 4). The hydrological sections of the Renato River showed seasonal variations in flow rate and runoff velocity (Table 3 and Figures 6 and 7), with maximum peaks in section 1 (4.26 m^3 s^{-1}) and section 2 (38.54 m^3 s^{-1}) and in the wet-dry transition with a minimum point in section 1 (0.88 m^3 s^{-1}) and section 2 (8.87 m^3 s^{-1}) between August and October (dry-rain transition) (Figures 6 and 7). Similar dynamics occurred between liquid and solid flows since the peaks of solid flows in suspension and total followed the peaks of liquid flows during the evaluated period. In the rainy season, there is evidence of an increase in surface runoff and solid flows with an increase in the drainage area.

Table 2. Hydraulic characteristics of hydrological sections on the River Renato Watershed, Southern Amazon, Mato Grosso, Brazil.

Variables		Section 1	Section 2
Width (m)	W_{max}	6.00	22.00
	W_{med}	4.87	18.91
	W_{min}	4.20	17.80
Length (m)	L_{max}	2.40	3.74
	L_{med}	1.41	2.15
	L_{min}	1.10	1.18
Water Speed (m s^{-1})	S_{max}	0.26	0.47
	S_{med}	0.18	0.36
	S_{min}	0.10	0.24
Wet Area (m^2)	A_{max}	9.73	55.77
	A_{med}	6.92	40.90
	A_{min}	5.04	26.53
Flow (m^3 s^{-1})	Q_{Lmax}	2.76	32.31
	Q_{Lmed}	1.52	18.07
	Q_{Lmin}	0.54	6.65
Suspended-sediment concentration (mg L^{-1})	C_{ssmax}	7.13	8.96
	C_{ssmed}	4.60	4.38
	C_{ssmin}	2.32	2.09
Suspended-solid discharge (t d^{-1})	Q_{ssmax}	1.3327	10.5361
	Q_{ssmed}	0.5560	6.1187
	Q_{ssmin}	0.1584	2.5170
Entrained solid discharge (t d^{-1})	Q_{samax}	0.0174	0.3574
	Q_{samed}	0.0036	0.4140
	Q_{samin}	0.0045	0.0306
Total solid discharge (t d^{-1})	Q_{stmax}	1.3501	10.8935
	Q_{stmed}	0.5597	6.5327
	Q_{stmin}	0.1629	2.5476

where: max – maximum value of a single measurement obtained in the rainy season; min – minimum value obtained in the dry season; med – average value of all measurements over the period. * Evaluation period between 05/2019 and 11/2022.

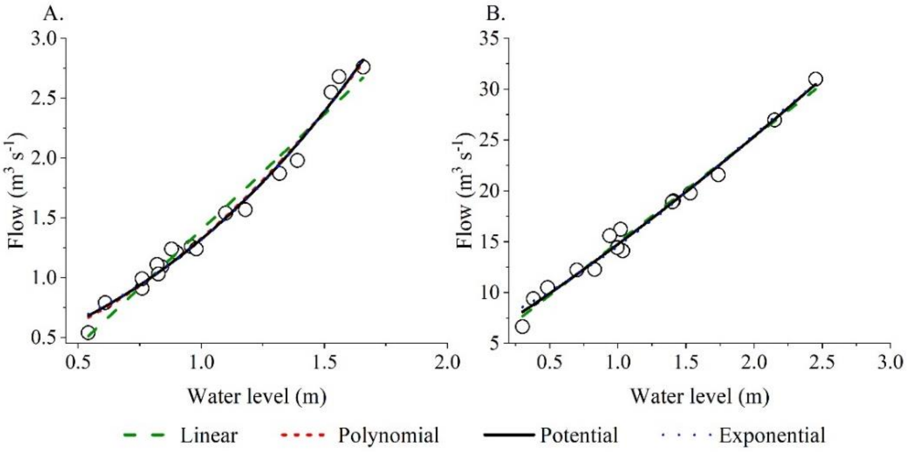

Figure 1. Adjusted flow rating curves for hydrological sections 1 (A) and 2 (B) of the River Renato Watershed, Southern Amazon, Mato Grosso, Brazil. *Evaluation period between 05/2019 and 11/2022.

Drag sediments showed little variation during the period evaluated for hydrological section 1 (Table 3 and Figure 6), unlike what was observed in hydrological section 2, in which a greater production of drag sediments was observed, with variations from 0.0273 to 1.3835 t d^{-1} between the dry and rainy seasons in the region (Table 3 and Figure 7).

Table 4. Coefficients of mathematical regression models used to fit the flow and sediment rating curves of the hydrological section 1 of the River Renato Watershed, Southern Amazon, Mato Grosso, Brazil.

Models	a	b	c	y_0	x_0	R^2	MBE	RMSE	dw	NSE	t
					Flow						
Linear	-0.53492	1.93429				0.9724	-0.1126	0.3587	0.8984	0.59	0.4176
Polynomial	0.27267	0.344	0.71251			0.9842	-0.1244	0.3505	0.9003	0.61	0.4702
Potential I	1.36031	1.38958				0.9806	-0.1199	0.3565	0.8995	0.59	0.4461
Potential II	0.37184	0.95397	1.85182			0.9839	-0.1245	0.3504	0.9003	0.61	0.4711
Potential III	0.07355	-1.46205	3.20581			0.9847	-0.1273	0.3495	0.9002	0.61	0.4835
Potential IV	0.647755	0.44304	-0.31193			0.9847	-0.1274	0.3495	0.9002	0.61	0.4836
Potential V	0.01544	3.80079		-0.20175	-2.34871	0.9849	-0.1278	0.3502	0.9001	0.61	0.4846
Potential VI	0.07355	3.20581			-1.46205	0.9847	-0.1273	0.3495	0.9002	0.61	0.4763
Potential VII	0.21312	2.63852				0.9846	-0.1259	0.3503	0.9003	0.61	0.4763
Exponential I	-1.5686	-0.61728				0.9844	-0.1256	0.3531	0.9000	0.60	0.4717
Exponential II	-1.5686	1.85388				0.9844	-0.1256	0.3531	0.9000	0.60	0.4716
Exponential III	-0.95166	1.21239				0.9826	-0.1351	0.3469	0.8988	0.61	0.5222
Exponential IV	-1.21854	1.69189	-0.19888			0.9844	-0.1278	0.3491	0.9001	0.61	0.4864
Exponential V	0.94852	1.21307		-0.75875	0.0454	0.9852	-0.1281	0.3497	0.9002	0.61	0.4863
		Mean values				0.9833	-0.1257	0.3512	0.8999	0.60	0.4748
		Standard derivation				0.0034	0.0050	0.0032	0.006	0.01	0.0231
					Suspended-solid discharge						
Linear	-0.1335	0.53934				0.9714	0.1595	0.3289	0.6338	-1.48	-0.8557
Polynomial	-0.11866	0.5182	0.0064			0.9715	0.1600	0.3301	0.6320	-1.49	-0.8571
Potential	0.5126	1.04024			0.20199	0.9716	0.1600	0.3307	0.6314	-1.50	-0.8559
Exponential	-2.55485	1.93163	-0.32589			0.9740	0.1608	0.3458	0.6214	-1.74	-0.8310
		Mean values				0.9721	0.1601	0.3339	0.6296	-1.55	-0.8499
		Standard derivation				0.0013	0.0006	0.0080	0.0056	0.12	0.0126
					Total solid discharge						
Linear	-0.13751	0.54554				0.9725	0.1620	0.3339	0.6273	-1.57	-0.8628
Polynomial	-0.11	0.50635	0.01186			0.9727	0.1630	0.3361	0.6240	-1.60	-0.8654
Potential	0.50272	1.0642			0.17936	0.9728	0.1629	0.3368	0.6236	-1.61	-0.8634
Exponential	-2.52918	1.90578	-0.31814			0.9750	0.1589	0.3453	0.6206	-1.75	-0.8226
		Mean values				0.9732	0.1617	0.3380	0.6239	-1.63	-0.8536
		Standard derivation				0.0012	0.0019	0.0050	0.0027	0.08	0.0207

Where: a, b, c, y_0 e x_0 – are coefficients adjusted by the regression models; R^2 – correlation coefficient; MBE - mean bias error, RMSE - root mean square error, dw - Willmott index of agreement.; NSE - Nash-Sutcliffe efficiency; t -

Student's t-test. Note: the equations highlighted in red were considered a reference for comparison with the other regression models and were also used to obtain models for solid flows.

Discussion

The Renato River is a natural and perennial watercourse, with continuous surface runoff flow throughout the year, low variations in the volume of water drained and in the transport of sediments between the regional water stations. In the evaluated period, a delay was observed between the periods of maximum liquid flow (December to May) and minimum (June to November), with greater lags with the increase in the drainage area (Figures 6 and 7). The rainy season, which begins in the third ten days of September, is responsible for underground and surface water recharge in this watershed; however, the speed of this recharge is dependent on the water demand (evapotranspiration) of the surface, the amount of precipitated water (Andrade et al., 2018; Rodrigues et al., 2020), the size of the drainage area, the shape, the slope, the drainage density (Wenzel et al., 2017; Santos et al., 2019), soil type, coverage and watershed management practices (Souza et al., 2019; Peixoto et al., 2020).

The Renato River watershed is little susceptible to flooding during the rainy season due to its elongated shape and regular drainage density (Table 2), which allow for a longer concentration time and good surface runoff capacity along the main watercourse to the basin outlet. The main drain is more sinuous as it approaches the mouth; this is because the sinuosity of the channel depends on the topography/relief of the basin's soil and in the region close to the mouth of the Renato River, the relief is more undulating.

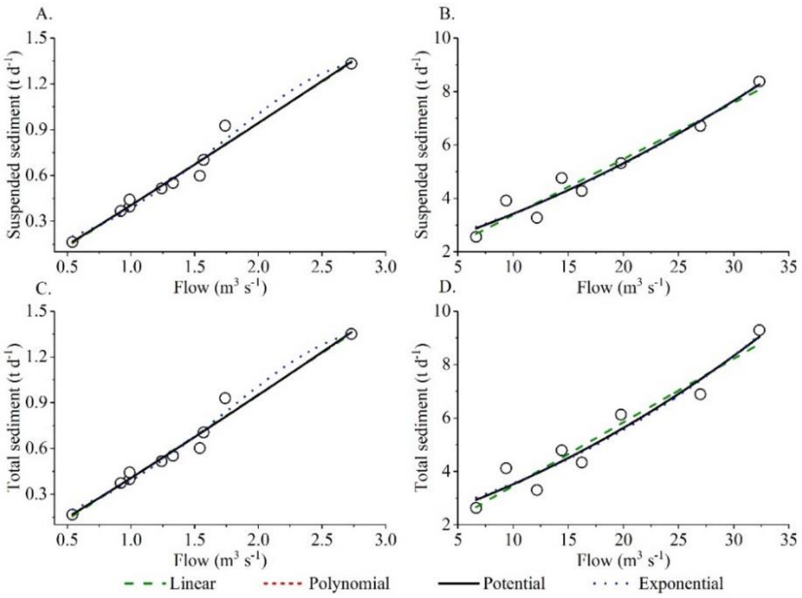

Figure 5. Adjusted suspended-solid and total solid discharge rating curves for hydrological sections 1 (A and C) and 2 (B and D) of the River Renato Watershed, Southern Amazon, Mato Grosso, Brazil. * Evaluation period between 05/2019 and 11/2022.

Table 5. Coefficients of mathematical regression models used to fit the flow and sediment rating curves of the hydrological section 2 of the River Renato Watershed, Southern Amazon, Mato Grosso, Brazil.

Models	a	b	c	y_0	x_0	R^2	MBE	RMSE	dw	NSE	t
Flow											
Linear	4.56446	10.37515				0.9823	0.5961	2.6514	0.9651	0.86	-0.1756
Polynomial	5.42337	8.70987	0.62691			0.9839	0.6993	2.9372	0.9593	0.83	-0.2005
Potential I	15.28869	0.72129				0.9705	0.4694	2.4082	0.9694	0.85	-0.1428
Potential II	5.70272	9.07141	1.11691			0.9833	0.6578	2.8258	0.9617	0.84	-0.1903
Potential III	6.91724	-0.83618	1.24657			0.9836	0.6805	2.8909	0.9603	0.83	-0.1958
Potential IV	3.94543	4.71828	-0.80219			0.9836	0.6810	2.8911	0.9603	0.83	-0.1960
Potential V	0.77714	1.94244		-23.212	-6.40451	0.9839	0.6996	2.9390	0.9592	0.83	-0.2006
Potential VI	6.91718	1.24657			-0.83619	0.9836	0.6805	2.8909	0.9603	0.83	-0.1958
Potential VII	5.80059	1.34289				0.9835	0.7017	2.9674	0.9586	0.82	-0.2007
Exponential I	46.32454	0.39933				0.9457	0.3655	2.3297	0.9712	0.89	-0.1117
Exponential II	46.32452	0.67077				0.9457	0.3654	2.3297	0.9712	0.89	-0.1117
Exponential III	2.11463	0.55086				0.9657	1.0569	4.5104	0.9190	0.59	-0.2741
Exponential IV	1.8893	0.90368	-0.11403			0.9808	0.5402	2.6921	0.9645	0.86	-0.1580
Exponential V	12.15522	7.80478		-62.7041	-13.4543	0.9840	0.7131	2.9749	0.9584	0.82	-0.2039
Mean values						0.9757	0.6362	2.8742	0.9599	0.83	-0.1827
Standard derivation						0.0139	0.1725	0.5263	0.0126	0.07	0.0418
Suspended-solid discharge											
Linear	1.27477	0.21022				0.9479	-2.3057	3.2929	0.5154	-0.96	2.4659
Polynomial	1.94755	0.12554	0.00216			0.9535	-2.3798	3.3675	0.5036	-1.05	2.5593
Potential	0.00106	2.1381			-33.6914	0.9535	-2.3999	3.3815	0.5029	-1.06	2.5838
Exponential	0.74642	0.05166	-0.00029			0.9531	-2.3960	3.3846	0.5006	-1.07	2.5812
Mean values						0.9520	-2.3703	3.3566	0.5056	-1.03	2.5476
Standard derivation						0.0027	0.0440	0.0431	0.0066	0.052	0.0555
Total solid discharge											
Linear	1.08427	0.238				0.9297	-2.5431	3.4159	0.5492	-0.92	2.5536
Polynomial	2.04131	0.11755	0.00307			0.9382	-2.6492	3.5268	0.5321	-1.05	2.6813
Potential	0.000473	2.34215			-34.992	0.9384	-2.6436	3.5205	0.5332	-1.04	2.6747
Exponential	0.77582	0.05133	-0.00022			0.9383	-2.9060	3.7089	0.5194	-1.27	3.0226
Mean values						0.9362	-2.6855	3.5430	0.5335	-1.07	2.7330
Standard derivation						0.0043	0.1549	0.1217	0.0122	0.14	0.2018

where: a, b, c, y_0 e x_0 – are coefficients adjusted by the regression models; R^2 – correlation coefficient; MBE - mean bias error, RMSE - root mean square error, dw - Willmott index of agreement.; NSE - Nash-Sutcliffe efficiency; t - Student's t-test. Note: the equations highlighted in red were considered a reference for comparison with the other regression models and were also used to obtain models for solid flows.

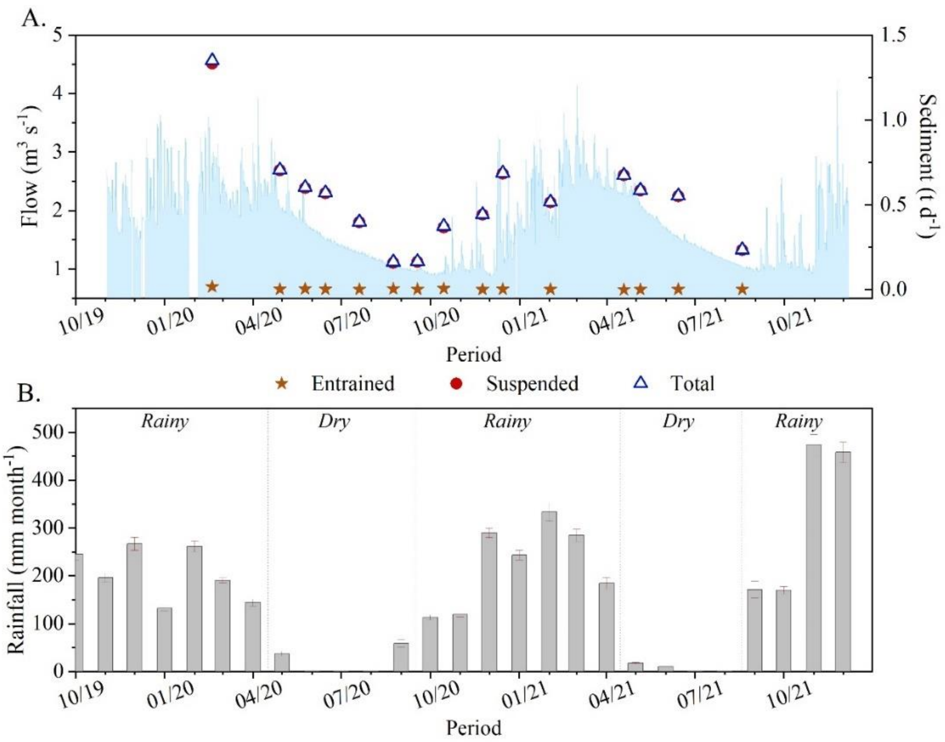

Figure 6. Flow (A) calculated by fitting the rating curve $y = a * |x - x_o|^b$ between 2019 and 2021, suspended-solid, entrained solid and total solid discharge (A) sampled monthly between 2020 and 2021 and rainfall (B) in hydrological section 1, of the River Renato Watershed, Southern Amazon, Mato Grosso, Brazil.

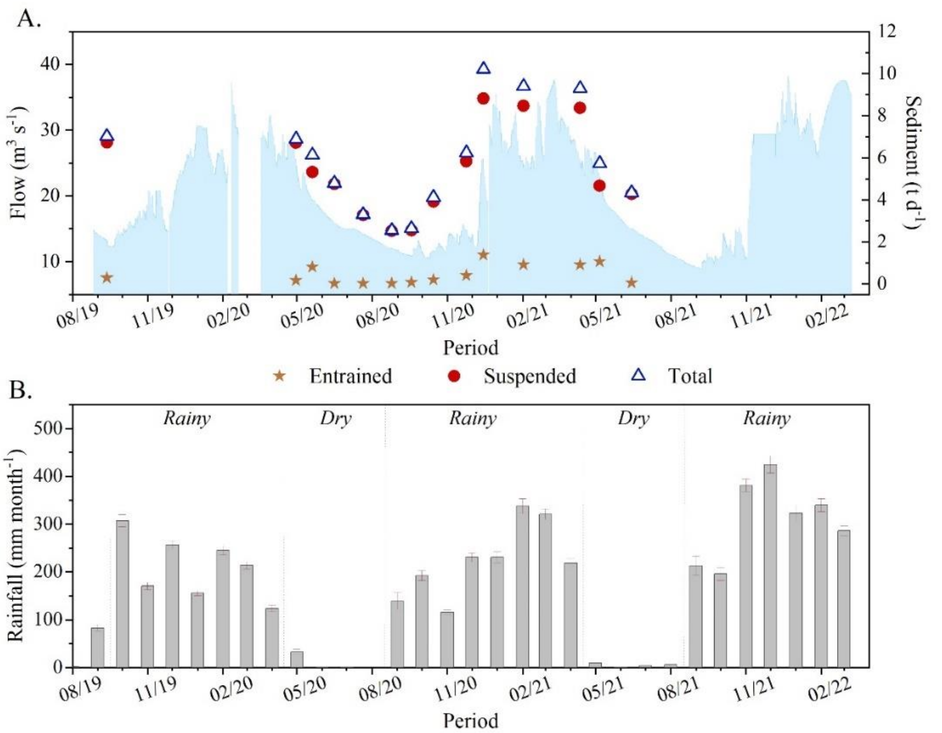

Figure 7. Flow (A) calculated by fitting the key curve $y = a * |x - x_o|^b$ between 2019 and 2021, suspended-solid, entrained solid and total solid discharge (A) sampled monthly between 2020 and 2021 and rainfall (B) in hydrological section 2, of the River Renato Watershed, Southern Amazon, Mato Grosso, Brazil.

The relief varies from flat (0 %) with greater occurrence in the source and middle region of the sub-basin to strongly undulating (30 %) in some points in the region close to the mouth of the Renato river, in these places with greater slope the native vegetation is still conserved. The slope of the watershed influences the speed of water flow over the soil and affects the storage capacity (Wenzel et al., 2017; Santos et al., 2019). The greater the slope of the basin associated with the absence of vegetation cover, the type of soil, the intensity of rainfall, among other factors, the lower the surface storage capacity, which increases the susceptibility to floods, subjecting the basin to degradation (Souza et al., 2019; Peixoto et al., 2020).

The regression models adjusted for constructing the net rating curves of the hydrological sections of the Renato River showed satisfactory statistical performance (Tables 4 and 5). This means that, regardless of the regression model, for these hydrological sections with low variations in water level throughout the year, the estimates of net discharge by the types of models evaluated will present good adjustments. The possible differences between the models become significant as the water level variation between minimum and maximum flows increases, thus allowing some of the variations proposed by the models to be more representative than the traditional potential model (Potential VI - Table 1).

This condition mentioned above can be better understood in fluviometric sections with great variation in level, as in the case of the Braco river basin (Acre), in which Tamwing et al. (2022) evaluating fluviometric sections with level variations greater than 20 meters between maximum and minimum flows, found net rating curves expressed by potential and polynomial equations with good adjustments for a period of 20 years. In this case, it is emphasized that the formation of historical series of liquid and solid flow data allows greater statistical security in the adjusted rating curves. However, the most representative types of regression models will depend on the hydraulic behavior of each evaluated section.

The dynamics of water and sediments in watersheds can be understood by morphometric characteristics (Wenzel et al., 2017; Coser & Grison, 2019; Santos et al., 2019), vegetative (Mendes et al., 2018; Andrade et al., 2018; Souza et al., 2019), edaphic (Almeida et al., 2019; Berihun et al., 2022) and climate (Sousa et al., 2020; Lopes et al., 2021).

The production of sediments in hydrographic basins, according to the classification described by Fonseca et al. (2022), varies from very low (<0.0027 t d^{-1} km^{-2}) to extremely high (>0.0548 t d^{-1} km^{-2}). Thus, the production of sediments in the Renato River is considered low, regardless of the season of the year, mainly due to the high presence of natural vegetation, which is around 69.0% (Figure 1).

The liquid and solid flows of the hydrological sections evaluated in the present study vary little, since they are small in drainage areas. As the drainage area increases, there are also increments in the variations of the hydrological characteristics, and this can influence the adjustments of the rating curves, making it necessary to evaluate other mathematical models that better represent the hydrological dynamics of the watercourse.

For the two hydrological sections of the Renato River, the solid rating curves adjusted by the different regression models showed unsatisfactory statistical performance with NSE < 0.50, with large overestimates and scattering, despite a high correlation between solid and liquid flows (Tables 4 and 5). This is due to the low number of sediment samplings for both hydrological sections of the Renato River. Thus, we emphasize the importance of continuing hydro-sedimentological monitoring, focusing mainly on sampling suspended sediments, since the slash sediments show little variation throughout the year, regardless of the fluviometric section.

Estimates of solid flows based on net flows, for short series of data have shown good adjustments and statistical performances, as in the cases observed by Peixoto et al. (2020) for the Jordão River (in the mesoregion of Triângulo Mineiro and Alto Paranaíba – MG) with the potential model (1 year of data), Simioni et al. (2021) for the Caiabi River (in Vera – MT) with the exponential model (2 years of data) and Sirqueira et al. (2022) for the Caiabi River (fluviometric section with smaller drainage area) with the polynomial model (1 year of data). With little more than one year of data, the present study did not present adjustments with satisfactory statistical performance for estimates of suspended solid and total flow based on the liquid flow, regardless of the regression model.

Considerações finais

The Renato River watershed has an elongated shape, flat to strongly undulating relief, regular drainage density and the main watercourse is more sinuous as it approaches the outlet, with low susceptibility to flooding.

The linear, polynomial, potential and exponential regression models adequately adjusted the net rating curves of the hydrological sections of the Renato river hydrographic sub-basin. They can be adjusted for other fluviometric sections, which present small variations between maximum and minimum flows.

For the Renato River watershed, the linear, polynomial, potential and exponential regression models did not present good estimates of the solid flow in suspension and total with data restriction, being necessary, the continuity of the hydro-sedimentological monitoring for new adjustments of the solid rating curves, with samples mainly of the sediments in suspension, since the sediments of drag show little variation throughout the year.

Acknowledgments

This article was funded by the Coordenação de Aperfeiçoamento de Pessoal de Nível Superior - Brazil (CAPES) and Agência Nacional de Águas e Saneamento Básico (ANA), Financing Code – 001 and Process 88887.144957/2017-00. To the Conselho Nacional de Desenvolvimento Científico e Tecnológico (CNPq) for the support with scientific initiation scholarships and productivity scholarship (Process 308784/2019-7). To the 3rd Comarca de Justiça Cível de Sinop for the CBH Monitora Project's financial support and the Comitê dos Afluentes da Margem Direita do Alto Teles Pires.

Referências

Agritempo. Agrometeorological Monitoring System: Meteorological Station. (2022). Available online: https://www.agritempo.gov.br/agritempo/jsp/PesquisaClima/index.jsp?siglaUF=MT. Accessed: 20 October 2022).

Almeida, W. S., Carvalho, D. F., Pereira, F. A. C., Rouws, J. R. C. (2019). Sediment production and soil water infiltration under different simulated rainfall characteristics. Revista Brasileira de Engenharia Agrícola e Ambiental , 23(8), 572-57. http://dx.doi.org/10.1590/1807-1929/agriambi.v23n8p572-578

Alves, M. A. B., Borella, D. R., Luz, C. C. da S., Castagna, D., Silva, W. C. da, Silva, A. F. da, Almeida, F. T. de, Souza, A .P de. (2022). Soil classes in the Caiabi and Renato Rivers basins, tributaries of the Teles Pires river in the south of the Amazon. Nativa, 10(3), 431-448. https://doi.org/10.31413/nativa.v10i3.14192

ANA - Agência Nacional De Águas E Saneamento Básico. Topobathymetric and geodetic surveys applied in the National Hydrometeorological Network (NHN). (2021). National Water and Basic Sanitation Agency, Geological Survey of Brazil. Brasília: ANA, 118p.

Andrade, E. M., Rodrigues, R. N., Palácio, H. A. Q., Brasil, J. B., Filho, J. C. R. (2018). Hydrological responses of a watershed to vegetation changes in a Tropical Semiarid region. Revista Caatinga, 31(1), 161-170.

Andrietti, G., Freire, R., Amaral, A. G., Almeida, F. T. de, Bongiovani, M. C., Schneider, R. M. 2016. Water quality index and eutrophication indices of Caiabi River, MT. Revista Ambiente & Água, 11(1) 162-175. https://doi.org/10.4136/ambi-agua.1769

Berihun, M. L., Tsunekawa, A., Haregeweyn, N., Tsubo, M., Fenta, A. A., Ebabu, K., Sultan, D., Dile, Y. T. (2022). Reduced runoff and sediment loss under alternative land capability-based land use and management options in a sub-humid watershed of Ethiopia. Journal of Hydrology: Regional Studies, 40, e100998. https://doi.org/10.1016/j.ejrh.2022.100998

Carvalho, N. O. (2008). Practical hydrosedimentology. 2ª ed. Rio de Janeiro: Interscience, 599p.

Coser, E. & Grison, F. (2019). Hydraulic geometry in a stream reach applying HEC-RAS. Revista Brasileira de Geomorfologia, 20(4), 691-706. https://doi.org/10.20502/rbg.v20i4.1512.

Fonseca, C. A. B. da, Al-Ansari, N., Silva, R. M. da, Santos, C. A. G., Zerouali, B., Oliveira, D. B. de, Elbeltagi, A. (2022). Investigating Relationships between Runoff–Erosion Processes and Land Use and Land Cover Using Remote Sensing Multiple Gridded Datasets. International Journal of Geo-Information, 11(272), 1-27. https://doi.org/10.3390/ijgi11050272

Groppo, J. D., Salemi, L. F., Moraes, J. M., Trevisan, R., Martinelli, L. A. (2019). Hydrological processes in watershed within the State Park of Serra do Mar, Santa Virgínia stewardship. Ciência Florestal, 29(2), 595-606. https://doi.org/10.5902/1980509831323

IBGE - Instituto Brasileiro de Geografia e Estatística. Continuous cartographic bases [database]. (2017). Available online:https://downloads.ibge.gov.br/index.htm. Accessed: 5 May 2022.

IBGE - Instituto Brasileiro de Geografia e Estatística. 2021. Basins and hydrographic divisions of Brazil. (2021). 160p. Available online:https://biblioteca.ibge.gov.br/index.php/biblioteca-catalogo?view=detalhes&id=2101854. Accessed: 3 March 2022.

IBGE - Instituto Brasileiro de Geografia e Estatística. State of Mato Grosso: Pedology (Exploratory Soil Map, scale 1:1.500.000). (2021). 1p. Available online:https://mapas.ibge.gov.br/tematicos/solos. Accessed: 3 April 2022.

Kraeski, A., Almeida, F. T., Carvalho, T. M., Souza, A. P. (2022). Identification of land use conflicts in Permanent Preservation Area in a Brazilian Amazon sub-basin. Sociedade & Natureza, 35, e65951. https://doi.org/10.14393/SN-v35-2023-65724

Lepesqueur, J., Hostache, R., Martínez-Carreras, N., Montargès-Pelletier, E., Hissler, C. (2019). Sediment transport modelling in riverine environments: on the importance of grain-size distribution, sediment density, and suspended sediment concentrations at the upstream boundary. Hydrology and Earth System Science, 23, 3901-3915. https://doi.org/10.5194/hess-23-3901-2019

Lopes, T. R., Zolin, C. A., Mingoti, R., Vendrusculo, L. G., Almeida, F. T de, Souza, A. P., Oliveira, R. F. de, Paulino, J., Uliana, E. M. (2021). Hydrological regime, water availability and land use/land cover change impact on the water balance in a large agriculture basin in the Southern Brazilian Amazon. Journal of South American Earth Sciences, 108, e103224. https://doi.org/10.1016/j.jsames.2021.10322

MapBiomas. MapBiomas Collection 6.0: Land Cover and Land Use Maps. (2020). Available online: https://mapbiomas.org/
colecoes-mapbiomas-1?cama_set_language=pt-BR (accessed on 7 July 2022).

MapBiomas. “Project MapBiomas – Mapping the water surface in Brazil: The dynamics of the water surface in the Brazilian territory (Collection 1). (2021). Available online: https://mapbiomas.org/o-projeto. Accessed: 5 May 2022).

Marinho, R. R., Filizola Junior, N. P., Martinez, J. M., Harmel, T. O. (2022). Suspended sediment transport estimation in Negro River (Amazon Basin) using MSI/Sentinel-2 data. Revista Brasileira de Geomorfologia, 23, 1174-1190. http://dx.doi.org/10.20502/rbg.v23i1.2076

Mello, C. R. de. Hydrology: principles and applications in agricultural systems. (2013). Lavras: Publishing Company UFLA, 455p.

Mendes, N. G. De S., Cecílio, R. A., Zanetti, S. S. 2018. Forest Coverage and Streamflow of Watersheds in the Tropical Atlantic Rainforest. Revista Árvore, 42(2), 1-10. http://dx.doi.org/10.1590/1806-90882018000200004

Moriasi, D. N., Arnold, J. G., Liew, V. W. M., Bingner, R. L., Harmel, R. D., Veith, T. L. (2007). Model evaluation guidelines for systematic quantification of accuracy in watershed simulations. Transactions of the ASABE, 50, 885-900.

Peixoto, R. A. O., Pereira, C. E., Salla, M. R., Alamy Filho, J. E., Nishimura, A. (2020). Determination of the liquid and solid discharge ratio and analysis of factors influencing the dynamics of sediment transport in the Jordão River Watershed (UPGRH-PN 1). Engenharia Sanitária e Ambiental, 25(6), 921-931. https://doi.org/10.1590/S1413-4152202020180137

Peixoto, R. A. O., Pereira, C. E., Salla, M. R., Alamy Filho, J. E. (2021). Study of sediment transport in the Jordão River, located in the mesoregion of the Triângulo Mineiro-MG. Acta Scientiarum Technology, 43, e51714. https://doi.org/10.4025/actascitechnol.v43i1.51714

Rodrigues, A. L., Villa, P. M., Rodrigues, A. C., Mata, R. A., Martorano, L. C. (2020). Water balance of a microbasin in atlantic forest: implications for the water resources management. Revista Brasileira de Climatologia, 26, 614-628. https://doi.org/10.1590/1413-7054202145008421

Santos, I., Fill, H. D., Sugai, M. R. V. B., Buba, H., Kishi, R. T., Marone, E., Latert, L. F. (2001). Applied hydrometry. Curitiba, Institute of Technology for Development, 372p.

Santos, L. L. dos, Ribeiro, V. de O., Diodato, J. O. (2019). Morphometry of Hydrographic Basins Placed in the Urban Area of Dourados - MS – Brazil. Ra’ega – O espaço geográfico em análise, 46(3), 75-87. http://dx.doi.org/10.5380/raega.v46i3.67039

Simioni, C. F., Almeida, F. T. de, Zolin, C. A., Uliana, E. M., Souza, A.P., Marques, A. (2021). Solid discharge in a microbasin of the amazon region. Ciência & Natura, 43, e73. https://doi.org/10.5902/2179460X64223

Sirqueira, E. S., Almeida, F. T. de, Araújo, H. B., Zolin, C. A., Carvalho, G. A., Paulista, R. S. D., Silva, A. F. da, Borella, D. R. (2022). Net flow, suspended sediments and turbidity in the Caiabi River microbasin, in the Cerrado-Amazon ecotone. Nativa, 10(4), 525-532. https://doi.org/10.31413/nativa.v10i4.13961

Sousa, M. M. M., Palácio, H. A. Q., Andrade, E. M., Ribeiro Filho, J. C., Moura, M. M. S. (2020). Determinant pluviometric characteristics of sediment transport in a catchment with thinned vegetation in the Tropical Semiarid. Revista Caatinga, 33(3), 785-793. https://doi.org/10.1590/1983-21252020v33n322rc

Souza, A. P., Mota, L. L., Zamadei, T., Martim, C. C., Almeida, F. T. de, Paulino, J. (2013). Climate Classification and Climatic Water Balance in Mato Grosso State, Brazil. Nativa, 1(1), 34-43. http://dx.doi. org/10.14583/2318-7670.v01n01a07

Souza, A. P., Silva, A. C., Tanaka, A. A., Uliana, E. M., Almeida, F. T. de, Klar, A. E., Gomes, A. W. A. (2017). Global radiation by simplified models for the state of Mato Grosso, Brazil. Pesquisa Agropecuária Brasileira, 52(4), 215-227. https://doi.org/10.1590/S0100-204X2017000400001

Souza, V. A. S., Rotunno Filho, O. C., Moreira, D. M., Rudke, A. P., Sá, M. R. T. (2019). Dynamics of deforestation in Amazonia and its impacts in hydrology: Machadinho River basin – Rondônia/Brazil. Ciência Florestal, 29(3), 1004-1018. https://doi.org/10.5902/1980509835333

Spera, S. T., Magalhães, C. A. de S., Baldoni, A. B., Calderano, S. B. (2019). Pedological characterization at places of occurrence of natural populations of Brazil nuts in the State of Mato Grosso. Nativa, 7(2), 145-161. http://dx.doi.org/10.31413/nativa.v7i2.6502

Stinghen, C. M. & Mannich, M. (2022). Overview of critical basin management in Brazil. Revista de Gestão de Água da America Latina, 19, e13. https://doi.org/10.21168/rega.v19e13

Tamwing, D. S., Montefusco, C., Irureta, O. O. A., Mesquita, A. A., Serrano, R. O. P., Moreira, J. G. V. (2022). Quota-flow ratio and key-curve adjustment: case study in the hidrographic basin of the Acre River (Acre, Brazil). Revista Ibero-Americana de Ciências Ambientais, 13(1), 129-140. http://doi.org/10.6008/CBPC2179-6858.2022.001.0011

Uliana, E. M., Souza, L. G. da S., Silva, D. D. da, Souza, A. P., Almeida, F. T. de, Araújo, H. B. (2016). Hydrological regionalization of flows for the medium and upper Teles Pires River – MT, Brazil. Revista de Ciências Agrárias, 59(4), 333-338. http://dx.doi.org/10.4322/rca.2240

Wang, X., Zhao, X., Zhang, Z., Yi, L., Zuo, L., Wen, Q., Liu, F., Xu, J., Hu, S., Liu, B. (2016). Assessment of soil erosion change and its relationships with land use/cover change in China from the end of the 1980s to 2010. Catena, 137, 256-268. https://doi.org/10.1016/j.catena.2015.10.004

Wenzel, D. A., Uliana, E. M., Almeida, F. T. de, Souza, A. P. de, Mendes, M. A. dos S.A., Souza, L. G. da S. (2017). Physiographic characteristics of the medium and upper Teles Pires River sub-basins, Mato Grosso, Brazil. Revista de Ciências Agro-ambientais, 15(2), 123-131.

Zhanga, S., Lia, Z., Houa, X., Yib, Y. (2019). Impacts on watershed-scale runoff and sediment yield resulting from synergetic changes in climate and vegetation. Catena, 179, 129-138. https://doi.org/10.1016/j.catena.2019.04.007

Ziembowicz, M. M., Marchesan, J., Baratto, J., Alba, A., Silva, R. R., Pereira, R. S. (2018). Geotechnology applied in the analysis of the impacts on the land use and land cover caused by the construction of a hydroelectric plant. Ciência & Natura, 40, e17. https://doi.org/10.5902/2179460X29847

Zolin, C. A., Paulino, J., Silva Matos, E., Magalhães, C. A. S., Almeida, F. T. de, Souza, A. P., Mingoti, R. (2016). Soil and water losses under crop-forest integration and in soybean-corn succession. Pesquisa Agropecuária Brasileira, 51(9), 1223-1230. https://doi.org/10.1590/S0100-204X2016000900022